Analytical calculation of the mean time spent by photons inside an absorptive inclusion embedded in a highly scattering medium

Victor Chernomordik
David W. Hattery
National Institutes of Health
National Institute of Child Health and Development
Bldg. 12A, Rm. 2041
9000 Rockville Pike
Bethesda, Maryland 20892-5626

Israel Gannot
Tel-Aviv University
Biomedical Engineering Department
Faculty of Engineering
Tel-Aviv 69978, Israel

Giovanni Zaccanti
Università degli Studi di Firenze and INFM
Dipartimento di Fisica
Via G. Sansone 1, 50019 Sesto Fiorentino
Firenze, Italy

Amir Gandjbakhche
National Institutes of Health
National Institute of Child Health and Development
Bethesda, Maryland 20892-5626

Abstract. The mean time spent by photons inside a nonlocalized optically abnormal embedded inclusion has been derived analytically. The accuracy of the results has been tested against Monte Carlo and experimental data. We show that for quantification of the absorption coefficient of absorptive inclusions, a corrective factor that takes into account the size of the inclusion is needed. This finding suggests that perturbation methods derived for very small inclusions which are used in inverse algorithms require a corrective factor to adequately quantify the differential absorption coefficient of nonlocalized targets embedded in optically turbid media. © *2002 Society of Photo-Optical Instrumentation Engineers.* [DOI: 10.1117/1.1481900]

1 Introduction

The highly scattering nature of tissue prevents embedded inclusions from being adequately resolved in optical images.[1] Hence, differing theoretical constructs have been proposed to separate the effects of scattering and absorption, enabling one to quantify optical coefficients as a spectroscopic signature of abnormal tissue embedded in thick, otherwise normal tissue. The most widely used of these theoretical constructs are the diffusion-like models based on the diffusion approximation of the transport equation and models based on random walk theory (RWT).[2] These theories can be used to fit experimental data and retrieve optical properties or can be implemented in computationally intensive inverse algorithms to map the optical properties of the tissue. However, it is well established that those inverse algorithms are ill posed. Thus, results obtained from such algorithms often differ from nominal values of the medium under interrogation. For this reason, we believe it is necessary to test the forward problem with independent data sets obtained from actual experiments or Monte Carlo (MC) simulations in which the parameters involved (e.g., size of the target or the amplitude of the perturbations) are varied. This allows one to test the robustness of the theory and therefore apprehend its limits. If inverse algorithms are applied to actual experiments in the absence of such tests, the origin of observed discrepancies between the nominal values and the constructed values will be unclear: are the discrepancies due to the ill poseness of the inverse method or the inaccuracy of the theory?

For example, we have used RWT to derive the absorptive perturbation kernel of a small abnormal inclusion embedded in a tissue-like turbid medium.[3] However, when we have used the standard method of integrating our perturbation kernel over the volume of a nonlocalized target, we found that simple extrapolation (i.e., integration over the volume) of the perturbation method yields inaccurate results for large inclusions. This was the motivation for deriving a corrective factor which takes into account effects of each absorptive unit (e.g., voxel) on other units and vice versa. In other words, assuming that each voxel is independent can result in significant errors. It should be noted that the perturbation kernel derived from RWT is similar to that obtained from the diffusion approximation.[3] Hence, the present work could possibly solve discrepancies encountered in reconstructed images using diffusion approximation-based approaches.

In time-resolved transillumination experiments, the temporal distribution of photon paths inside the tissue is critically dependent on the optical coefficients of the tissue background, as well as those of the abnormal target(s) under investigation. The mean time that photons have spent inside an abnormal target can be seen as a quantitative parameter for imaging purposes. It is worth noting that this parameter was first introduced theoretically as a "photon hitting density" by Schotland, Haselgrove, and Leigh.[4] The authors reduced the problem of calculating the photon hitting density to that of determining the diffusion Green's functions. However, no comparisons of this model with experimental data or Monte Carlo simulations have been published. Though it was not

Address all correspondence to Victor Chernomordik. Tel: 301-435-9236; Fax: 301-435-9236; E-mail: vchern@helix.nih.gov
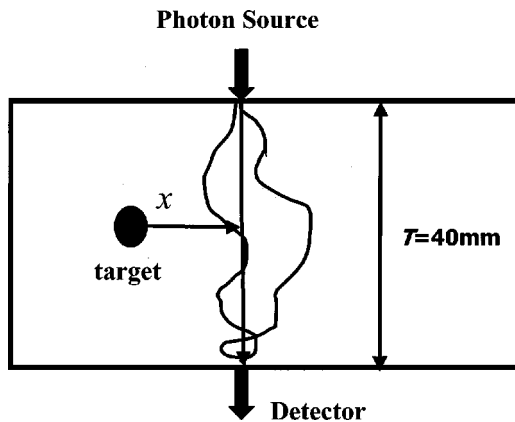
Fig. 1 Geometric scheme assumed for theoretical model, Monte Carlo simulations, and corresponding experimental setup.

analyzed, the factor would be most significant in the case of relatively large, nonlocalized absorbing targets.

Recently, Zaccanti et al.[5] have proposed a method to measure the mean flight time $\langle t_i \rangle$ spent by photons inside a given volume of a highly diffusing medium. The authors have substantiated their approach with Monte Carlo simulations and experiments. In the most recent paper by the same group,[6] Monte Carlo simulations and experimental data were used to assess the accuracy of a perturbation approximation to the diffusion model for scattering and absorbing inhomogeneities.

Using the data, obtained from those researchers at the University of Florence, we show that the time dependent contrast functions proposed by Gandjbakhche et al.[7] could provide a direct and quantitative analysis of the mean time spent inside an abnormal inclusion. Similarly, Monte Carlo simulations and experiments aimed at an estimate of $\langle t_i \rangle$ can substantiate assumptions of the random walk (RW) model of the time-resolved contrast functions $C_a(x, \Delta t)$ for absorptive inclusions,[3] in particular, for the case of relatively large non-localized inclusions.[8] To test the robustness of our analysis, we also present in Sec. 3 an analysis of another independent set of time-resolved experimental data on absorptive inclusions of three different sizes obtained by Painchaud et al.[9]

2   Monte Carlo Simulations and Experimental Setup

Both experiments and Monte Carlo (MC) simulations employ the standard transillumination geometry for a highly scattering slab of thickness $T = 40$ mm (Figure 1). Sizes and amplitudes of absorptive perturbations were varied over a broad range. Setup details have been described recently elsewhere.[5] This setup has been employed to experimentally determine the mean time spent by photons inside a given inclusion before being detected on the side of the slab opposite the source. The measurements were made using the original methodology of the paper,[5] i.e., by measuring the relative variation of received time-resolved power $P(\Delta t, x, \mu_a + \delta \mu_a)/P(\Delta t, x, \mu_a)$ due to a small variation of the absorption coefficient $\delta \mu_a$ inside the inclusion

$$\langle t_i \rangle \left(\Delta t, x, \mu_a + \frac{\delta \mu_a}{2} \right) = - \frac{1}{c \, \delta \mu_a} \ln \left\{ \frac{P(\Delta t, x, \mu_a + \delta \mu_a)}{P(\Delta t, x, \mu_a)} \right\}. \tag{1}$$

Measurements have been carried out with the *CW* experimental setup fully described by Zaccanti et al.[5] A light beam emitted by a 5 mW He–Ne laser illuminates the center of the scattering cell containing a water suspension of intralipid. The transmitted light has been measured with an accuracy better than 0.3% using a bundle of fibers (diameter 3 mm, coaxial with the laser beam), a photomultiplier, and a lock-in amplifier. The absorption coefficient has been varied by inserting gels with calibrated optical properties inside the scattering cell. The gels, obtained by solidifying a water suspension of intralipid and India ink, had scattering properties almost identical to the suspension in the scattering cell. In all the experiments the optical properties of the background were $\mu_s' = 0.39 \pm 0.02$ mm^{-1}, and $\mu_a = 0.000\,38 \pm 0.000\,02$ mm^{-1}.

From MC simulations, both the temporal distribution of photons that have traveled from a source to a detector aligned on the opposite side of a slab, and the mean time spent by photons inside an absorptive inclusion have been derived. As is normally done, the trajectories of individual photons are simulated according to statistical rules that govern photon interactions within the medium. A sophisticated MC model based on scaling relationships that has been developed at the University of Florence[10] has also been used in this research. The simulation results reported here have been obtained by assuming an asymmetry factor g equal to zero, corresponding to Raleigh scatterers. Compared to the appropriately scaled results for nonzero g values, this approach produces only a very slight discrepancy near the source and for photons with very short flight times as expected.

3   Comparison of the RW Model With Experimental Data and MC Simulations

To compare the results of experiments and MC simulations with predictions of the RW model, we take advantage of an evident relationship between the mean time that photons spend inside the inclusion $\langle t_i \rangle (\Delta t)$ and the corresponding absorptive contrast $C_a(x, \Delta t)$ which is valid, if the extra optical depth inside inclusion $\Delta \tau = \Delta \mu_a c \langle t_i \rangle (\Delta t) \leqslant 1$ is

$$C_a(x, \Delta t) = \Delta \mu_a c \langle t_i \rangle (\Delta t), \tag{2}$$

where x is a shift of source-detector axis relative to the center of the inclusion, $\Delta \mu_a = \mu_a - \mu_a^{(0)}$ is a perturbation in the absorption coefficient corresponding to the abnormality, $\langle t_i \rangle (\Delta t)$ is the "time-resolved" mean time of flight spent by photons inside an inclusion [estimated for those photons that are to be detected on the other side of the slab after a time delay (Δt)], and c is the speed of light inside the medium. Absorptive contrast is a relative perturbation in detected intensity due to the presence of an absorptive inclusion.

RW formulas for $C_a(x, \Delta t)$ were recently derived and used for quantification of inclusions in tissue-like turbid slabs from time of flight experimental data.[3,8] Within the RW model framework, for a relatively small (size $d_i \ll L$, where L is slab thickness) abnormally absorbing inclusion, we can represent the inclusion by a set of N_a^3 independent absorbers located on

a cubic lattice with spacing $d_s = \sqrt{2}/\mu_s'$, where μ_s' is the transport-corrected scattering coefficient of the background. The contrast function is[8]

$$C_a(x, \Delta t) \approx \sum_{N_a^3} \eta_{\mathrm{eff}} \frac{W(x, \Delta t)}{p(\Delta t)}. \tag{3}$$

Here, $p(\Delta t)$, is the probability that, in the absence of the inclusion, an injected photon would reach the detector with time delay Δt, $W(x, \Delta t)$ is the probability that a photon, having visited the inclusion, will reach the detector with time delay Δt, and η_{eff} is the effective absorptivity of an elementary absorber[8]

$$\eta_{\mathrm{eff}} = \eta_0 \exp\left(\frac{-\Delta\mu_a \mu_s' d_i^2}{2} \right) = \eta_0 \exp\left(-\frac{\eta_0 (\mu_s' d_i)^2}{2} \right), \tag{4}$$

where $\eta_0 = \Delta\mu_a / \mu_s'$, $\Delta\mu_a = \mu_a - \mu_a^{(0)}$ is the perturbation of the absorption coefficient inside the inclusion with respect to the background. The exponential factor introduced on the right hand side of the phenomenological Eq. (4) is important when there is considerable additional absorption in the inclusion that reduces the effective photon intensity inside the inclusion compared to the unperturbed intensity. The index of exponent is equal to the product of the average number of RW steps inside an inclusion,[13] $N_{\mathrm{RW}}^{(0)} = (\mu_s' d_i)^2/2$, and the probability that, due to this additional absorption, a photon is absorbed at any lattice point inside the inclusion, η_0.

Taking into account that $N_a^3 = V(\mu_s'/\sqrt{2})^3$, and $d_i^2 = V^{2/3}$ for relatively small inclusions with extra optical depth τ due to nonzero absorption perturbation, $\Delta\mu_a$, not exceeding unity, $(\tau = \Delta\mu_a \mu_s' V^{2/3}/2 \lesssim 1)$, we obtain

$$\langle t_i(x, \Delta t)\rangle (\Delta\mu_a) = \frac{1}{c\mu_s'} \left\{ V \left[\frac{\mu_s'}{\sqrt{2}} \right]^3 \right\} \frac{W_{n+1}\left(\frac{\mu_s' x}{\sqrt{2}} \right)}{p_n}$$
$$\times \exp\left(-\frac{\Delta\mu_a \mu_s' V^{2/3}}{2} \right), \tag{5}$$

where V is inclusion volume, $n = c\Delta t \mu_s'$, and the number of steps corresponding to a time of flight Δt. W_{n+1}, the point spread function,[7,3] is assumed to be constant over the volume of the inclusion.

Comparison of Eq. (5) with the results of MC simulations shows very good agreement, as presented in Figures 2(a) and 2(b), for the case of small spherical inclusions of volume $V = 524 \ \mathrm{mm}^3$ and positive or negative absorption perturbations embedded halfway between the source and detector in a scattering medium with $\mu_s' = 0.5 \ \mathrm{mm}^{-1}$. Figures 2(a) and 2(b) correspond to the positive absorption perturbation of $\Delta\mu_a = 0.0025 \ \mathrm{mm}^{-1}$ $(\mu_a^{(0)} = 0)$ and the negative absorption perturbation of $\Delta\mu_a = -0.001 \ \mathrm{mm}^{-1}$ $(\mu_a^{(0)} = 0.001 \ \mathrm{mm}^{-1})$, respectively. The exponential factor in Eq. (5) accounts for a small difference ($\sim 6\%$) between the results of the MC simulations for two cases. It is worth noting that the RW model predicts an increase in $\langle t_i(x, \Delta t)\rangle$ with decreasing Δt for the shortest time delays, resulting from the index (number of RW
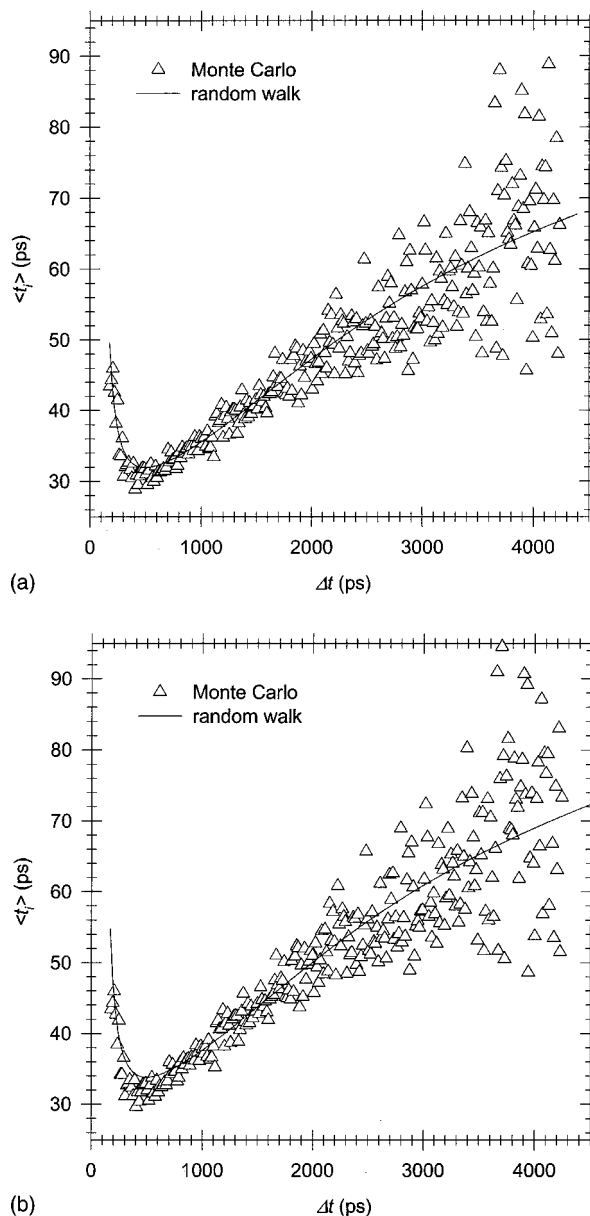

(a)

(b)

Fig. 2 Time-resolved mean time $\langle t_i\rangle(\Delta t)$ spent by photons inside an inclusion of the volume $V_i = 524 \ \mathrm{mm}^3$ with the absorption perturbation positioned midway between the source and detector (slab thickness $L = 40 \ \mathrm{mm}$, $\mu_s' = 0.5 \ \mathrm{mm}^{-1}$, refraction index $n = 1.33$); (a) $\mu_a^{(0)} = 0$, $\Delta\mu_a = 0.0025 \ \mathrm{mm}^{-1}$, (b) $\mu_a^{(0)} = 0.001 \ \mathrm{mm}^{-1}$, $\Delta\mu_a = -0.001 \ \mathrm{mm}^{-1}$.

steps) $n + 1$ of the probability W instead of n in the numerator of Eq. (5).[7] This kind of behavior at small Δt is not explained by the standard diffusion model of time-resolved contrast functions as discussed, for example, by Morin, et al.[11] Researchers using diffusion models generally introduce an *ad hoc* correction that is equivalent to one extra RW step.[11,12]

To further test the accuracy of the RW approach for estimates of absorptive contrast, we look at a correction factor for nonlocalized absorbing inclusions. We use the results of MC simulations and experiments that provide the time-integrated (*CW*) values of the mean time spent by photons inside an

absorptive inclusion. To quantitatively analyze these results, we take into account the reduction in the average number of RW steps inside an inclusion due to the background absorption $\mu_a^{(0)}$ (if it is not negligible). This reduction is derived, assuming, in accordance with the Central Limit Theorem, that the distribution of the random walk number of steps n_{RW} is Gaussian

$$f(n_{RW}) \propto \exp\left[- \frac{(n_{RW}-N_{RW}^{(0)})^2}{2N_{RW}^{(2)}} \right]. \quad (6)$$

The background absorption results in the following modification of Eq. (6):

$$\widetilde{f}(n_{RW}) \propto \exp\left[- \frac{(n_{RW}-N_{RW}^{(0)})^2}{2N_{RW}^{(0)2}} - \frac{\mu_a^{(0)}}{\mu_s'} n_{RW} \right]$$

$$\propto \exp\left\{ - \frac{\left[n_{RW}-N_{RW}^{(0)}\left(1 - \frac{\mu_a^{(0)}}{\mu_s'} N_{RW}^{(0)} \right) \right]^2}{2N_{RW}^{(0)2}} \right\} \quad (7)$$

and, hence, the following change in the average number of the random walk steps inside inclusion

$$N_{RW} = N_{RW}^{(0)}\left(1 - N_{RW}^{(0)}\frac{\mu_a^{(0)}}{\mu_s'} \right). \quad (8)$$

Finally, the corresponding formula for $\langle t_i \rangle_{cw}$ is obtained by a summation over the number of steps in the numerator and denominator of Eq. (5), and a modification of the index of the exponent

$$\langle t_i(x) \rangle(\Delta \mu_a) = \frac{1}{c\mu_s'}\left\{ V\left[\frac{\mu_s'}{\sqrt{2}} \right]^3 \right\} \frac{\Sigma_n W_{n+1}\left(\frac{\mu_s' x}{\sqrt{2}} \right)}{\Sigma_n p_n}$$

$$\times \exp\left\{ - \frac{\Delta \mu_a V^{2/3}\mu_s'}{2}\left(1 - \frac{\mu_a^{(0)}V^{2/3}\mu_s'}{2} \right) \right\}. \quad (9)$$

In Figure 3 we present a comparison of the calculated dependency of $\langle t_i \rangle_{cw}$ on the lateral shift x of the inclusion center relative to the source-detector axis with the experimentally observed values and results from MC simulations presented by Zaccanti et al.[5] Agreement between the model and data proves to be good. It is worth noting that the shape of the lateral distribution is close to Gaussian as has been previously shown.[13]

Figure 4 shows $\langle t_i \rangle_{cw}$ as a function of the background absorption coefficient $\mu_a^{(0)}$. MC simulations for this case confirm the RW predictions, illustrating the accuracy of the Green functions estimates based on the RW model.

Two more dependencies of the mean time $\langle t_i \rangle_{cw}$ on the parameters of the inclusion itself, i.e., the target volume, V, and the amplitude of absorption perturbation, $\Delta \mu_a$, are presented in Figures 5 and 6, respectively. Figure 5 shows the match between the new theory, MC simulations, and experimental data.[5] In Figures 6(a) and 6(b), only MC results were available. Figure 6(a) corresponds to the case without the
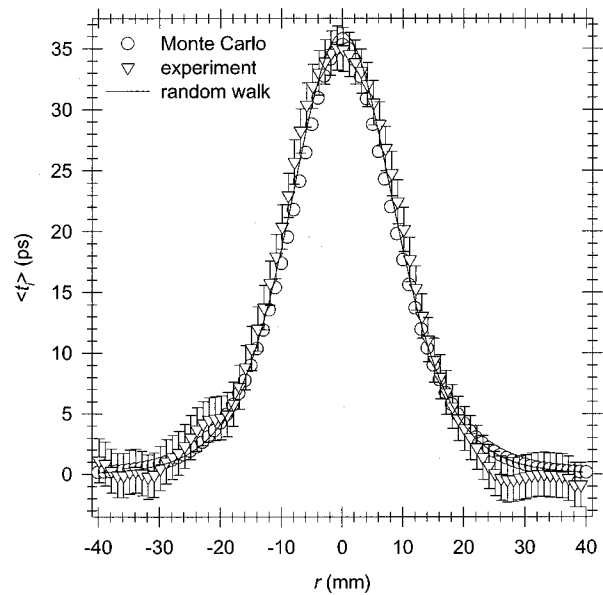

Fig. 3 Lateral distribution of the CW mean time $\langle t_i \rangle(x)$, spent by photons inside an inclusion of the volume $V_i = 592$ mm^3 with the absorption perturbation $\Delta \mu_a = 0.0069$ mm^{-1} positioned in the slab midplane; x is the distance between the inclusion center the source-detector axis.

background absorption ($\mu_a^{(0)} = 0$) and positive absorption perturbations $\Delta \mu_a$, while Figure 6(b) corresponds to the case of $\mu_a^{(0)} = 0.02$ mm^{-1} and the broader range of perturbation amplitudes, including negative values $\Delta \mu_a$. For relatively small values of inclusion volume and/or absorption perturbation, both relationships are well described by the RW formulas for quasipoint absorptive inclusions,[3] while for larger abnormali-
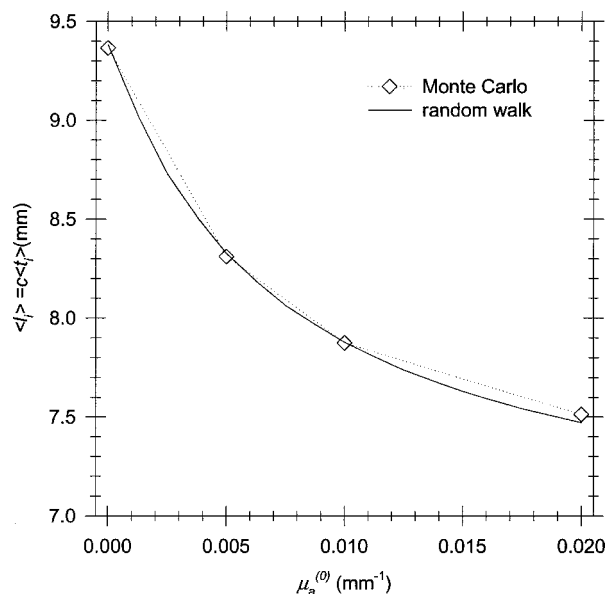

Fig. 4 Dependence of the CW mean time $\langle t_i \rangle_{cw}$ on the background absorption coefficient $\mu_a^{(0)}$ ($\mu_s' = 0.5$ mm^{-1}, inclusion volume $V_i = 524$ mm^3, absorption perturbation $\Delta \mu_a = 0.000\,05$ mm^{-1}).
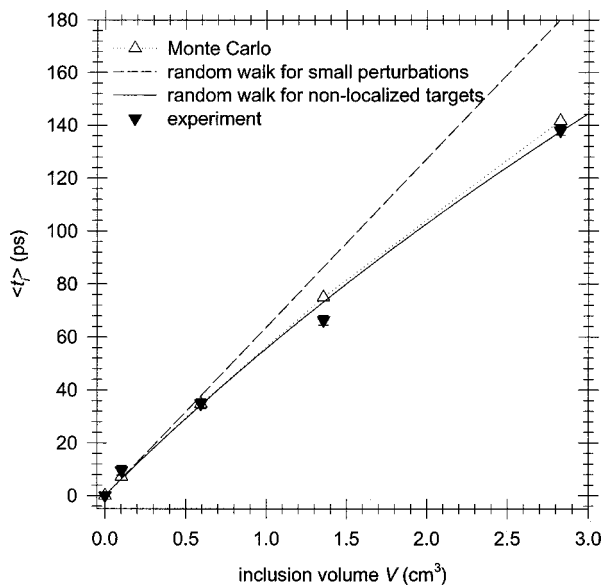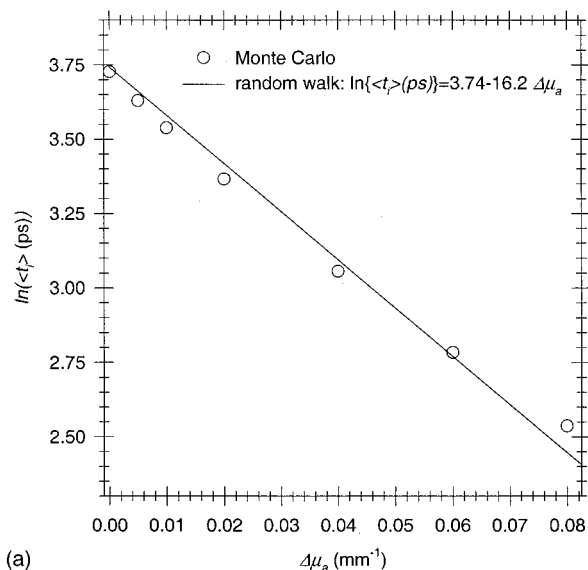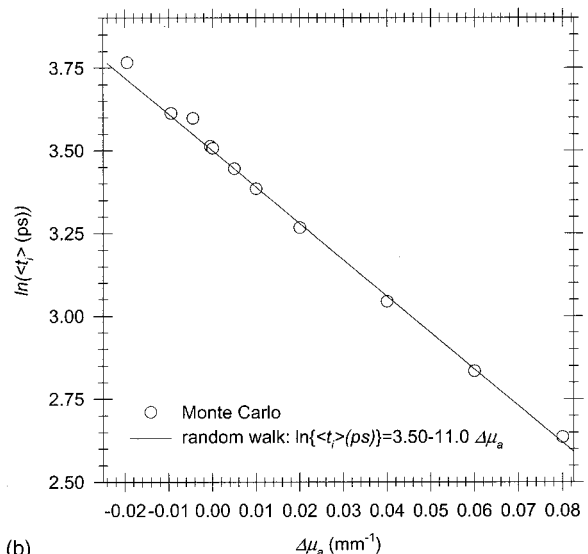
Fig. 5 Dependence of the CW mean time $\langle t_i \rangle_{cw}$ on the inclusion volume V (absorption perturbation $\Delta\mu_a = 0.0069$ mm^{-1}); both the experimental data and results of MC simulations for the same conditions are shown.

ties good agreement is only achieved if one uses Eq. (9) with the exponential correction factor [for small $\mu_a^{(0)}$ this factor is presented in Eq. (4)].

Additional comparisons between the results of MC simulations for the mean photon pathlengths $\langle l_i \rangle_{CW} = c\langle t_i \rangle_{CW}$ inside the absorptive inclusion of the volume $V = 524$ mm^3 with predictions of the RW model [Eq. (9)] are presented in Table 1 for a wide range of $\mu_a^{(0)}$ and $\Delta\mu_a$. Errors from the RW expression were less than 6% (and generally much less) for optical depths $\tau \lesssim 1$. The error increases up to $\sim 10\%-12\%$ for $\tau \approx 1.3$ (the last row of Table 1). The dependence of absorptive contrast amplitude (which is proportional to the mean time spent inside the inclusion $\langle t_i(t) \rangle$) on the size of the inclusion is further tested by using independent experimental data from Painchaud et al.[9] Time-resolved contrast functions for three similar, purely absorptive inclusions (cylinders with equal diameter and height d) that differ only in size ($d = 3.6, 5.0, 7.0$ mm) were presented. All measurements were reported to have been made in transillumination geometry with the inclusion halfway between the source and detector in a slab of thickness $L = 20$ mm (scattering and absorption coefficients of the background were $\mu_s' = 1.13$ mm^{-1} and $\mu_a^{(0)} = 0.002$ mm^{-1}). In Figure 7(a) we present experimental contrast amplitudes as a function of the cubed size of the inclusion for the time delay $\Delta t = 1000$ ps. As expected, for the relatively large inclusion size $d = 7.0$ mm when a simple perturbation analysis [corresponding to no correction as in Eq. (3) with $\eta_{eff} = \eta_0 = \Delta\mu_a/\mu_s'$] fails, absorptive contrast deviates from proportionality to the inclusion volume $V \propto d^3$. However, if one plots the same contrast amplitude as a function of parameter $Q = d^3 \exp(-\Delta\mu_a\mu_s' V^{2/3}/2)$ [Figure 7(b)] that takes into account the exponential correction factor in Eq. (4), the results are very close to linear and pass through the origin, as we expect from our model [see Eqs. (2) and (5)]. From these equations, taking into account that the RW ratio (W_n/p_n)

(a)

(b)

Fig. 6 Dependence of the CW mean time $\langle t_i \rangle_{cw}$ on the value of the absorption perturbation $\Delta\mu_a$ (inclusion volume $V = 524$ mm^3, background $\mu_s' = 0.5$ mm^{-1}); (a) $\mu_a^{(0)} = 0$, (b) $\mu_a^{(0)} = 0.02$ mm^{-1}.

≈ 0.16 for the number of steps, n, corresponding to $\Delta t = 1000$ ps, we were able to estimate μ_a inside the inclusion to be $\mu_a = 0.024 \pm 0.001$ mm^{-1} for all considered inclusion sizes. This is close to the nominal value of $\mu_a = 0.029$ mm^{-1}.

4 Discussion

Comparisons of theoretical predictions, based on the RW model, with MC simulations and two independent experimental data sets show that the mean time spent by photons inside an absorptive nonlocalized inclusion $\langle t_i \rangle$ cannot be accurately calculated without introducing a size-dependent exponential correction factor. This factor takes into account the probability of additional absorption of the photon at the RW lattice points inside the inclusion.

Table 1 Comparison of the results of Monte Carlo simulations for the mean photon pathlenghs inside the absorptive inclusion (CW mode) $\langle l_i \rangle_{CW} = c \langle t_i \rangle_{CW}$ with predictions of the random walk model [Eq. (9)].

$\mu_a^{(0)}$ (mm^{-1})	0.000			0.005			0.01			0.02		
	$\langle l_i \rangle_{CW}$ (mm)			$\langle l_i \rangle_{CW}$ (mm)			$\langle l_i \rangle_{CW}$ (mm)			$\langle l_i \rangle_{CW}$ (mm)		
$\Delta\mu_a$ (mm^{-1})	MC	RW	Error	MC	RW	Error	MC	RW	Error	MC	RW	Error
5.0×10^{-5}	9.37	9.38	0.1%	8.31	8.33	0.2%	7.88	7.88	0.0%	7.51	7.47	0.5%
5.0×10^{-3}	8.50	8.66	1.9%	7.67	7.73	0.8%	7.33	7.37	0.5%	7.07	7.07	0.0%
1.0×10^{-2}	7.76	7.98	2.8%	7.08	7.18	1.4%	6.83	6.88	0.7%	6.65	6.70	0.8%
2.0×10^{-2}	6.53	6.78	3.8%	6.09	6.18	1.5%	5.96	6.01	0.8%	5.91	6.00	1.5%
4.0×10^{-2}	4.79	4.90	2.3%	4.63	4.59	0.9%	4.62	4.57	1.1%	4.73	4.82	1.9%
6.0×10^{-2}	3.65	3.54	3.0%	3.61	3.40	5.8%	3.66	3.48	4.9%	3.84	3.87	0.8%
8.0×10^{-2}	2.85	2.56	10%	2.87	2.52	12%	2.95	2.65	10%	3.15	3.11	1.3%

Starting with the simple relationship between $\langle t_i \rangle$ and the corresponding absorptive contrast function [Eq. (2)], and using the RW derived formulas for mean time, $\langle t_i \rangle$, yields a practical framework in which the results of MC simulations and experiments may be compared. The excellent match between the simulations and experiments in this framework substantiates the use of this recently developed RW methodology[3,8] to quantify optical characteristics and sizes of abnormalities inside a turbid slab for relatively large (nonlocalized) absorptive inclusions.

This methodology is a multi-step analysis of time-resolved data. From images observed at differing flight times, we construct the time-dependent contrast functions, fit our theoretical expressions, and compute the optical properties of the background, and those of the inclusion along with its size. This method was successfully applied to reconstruct the optical characteristics and sizes of inclusions with increased scattering and/or absorption inside several independent tissue-like phantoms.[3,8] We used early time of flight data to estimate amplitudes of the scattering perturbations and sizes of the abnormality, while the long delayed photons are used to estimate absorption perturbations. Our exponential correction factor has been shown, for relatively large absorptive inclusions (both positive and negative), to improve the accuracy of estimated inclusion sizes and may be easily incorporated into our existing technique for analysis of absorptive contrast.[3] It
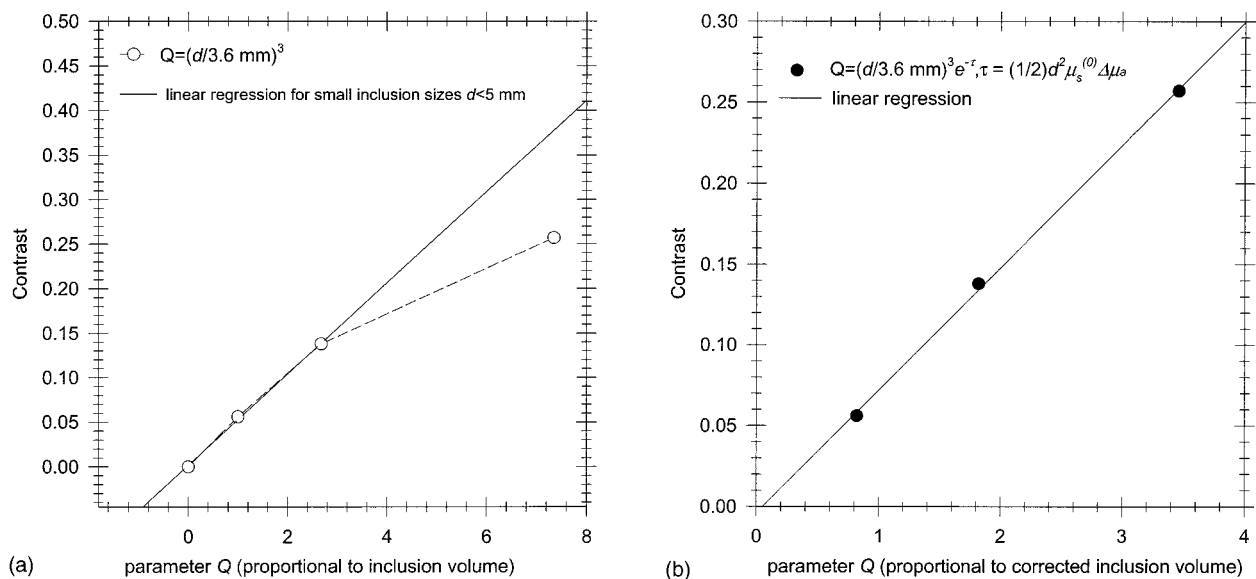

Fig. 7 Time-resolved contrast amplitude, as a function of size of inclusion; comparison with experimental data from Ref. 9 for three absorptive inclusions, positioned at the midplane of the highly scattering slab ($\mu_s' = 1.13$ mm^{-1}) of the thickness $L = 20$ mm that differ only in size ($d = 3.6, 5, 7$ mm). (a) Parameter Q related to size that corresponds to x axis of the graph, is simply d^3. (b) Parameter Q includes in addition to d^3 an exponential correction factor, described in Eq. (4).

is worth noting that our RW-based technique for analysis of the scattering perturbations[3,8] permits one to consider the case of the relatively large (nonlocalized) scattering inclusions.

Recently, in a pilot study, the same RW methodology was used to estimate optical parameters of the breast tumors from *in vivo* time-resolved data, obtained at two wavelengths.[14] From the absorption coefficients at both wavelengths blood oxygen saturation was found for the tumors and surrounding tissue. We plan to continue our work on quantification of tumor characteristics from *in vivo* time-resolved measurements in order to better characterize different types of abnormalities, and in particular, relatively large tumors.

It should be noted that in our approach, we do not try to retrieve the whole distributions of scattering and absorption coefficients over the tissue volume, as is usually the goal of diffuse optical tomography. Instead, we consider a more limited problem, i.e., to estimate under reasonable assumptions optical parameters and sizes of a single tissue abnormality with an absorptive and/or scattering perturbation inside a quasihomogeneous region of interest inside turbid tissue.

Our analysis suggests that for accurate quantification of the absorption coefficient of an embedded target, a corrective factor which is size dependent must be included in the forward model based on diffusion-like theories. Unfortunately, this inclusion makes the expression of absorptive contrast nonlinear. As a result, development of algorithms for diffuse optical tomography, already cumbersome, becomes more challenging.

References

1. J. C. Hebden, S. R. Arridge, and D. T. Delpy, "Optical imaging in medicine: I. Experimental techniques," *Phys. Med. Biol.* **42**, 825 (1997).
2. S. R. Arridge and J. C. Hebden, "Optical imaging in medicine: II. Modelling and reconstruction," *Phys. Med. Biol.* **42**, 841 (1997).
3. A. H. Gandjbakhche, V. Chernomordik, J. C. Hebden, and R. Nossal, "Time-dependent contrast functions for quantitative imaging in time-resolved transillumination experiments," *Appl. Opt.* **37**, 1973 (1998).
4. J. C. Schotland, J. C. Haselgrove, and J. S. Leigh, "Photon hitting density," *Appl. Opt.* **32**, 448 (1993).
5. G. Zaccanti, L. Alianelli, C. Blumetti, and S. Carraresi, "Method for measuring the mean time of flight spent by photons inside a volume element of a highly diffusing medium," *Opt. Lett.* **24**, 1290 (1999).
6. S. Carraresi, S. Tahani, F. Martelli, and G. Zaccanti, "Accuracy of a perturbation model to predict the effect of scattering and absorbing inhomogeneities on photon migration," *Appl. Opt.* **40**, 4622 (2001).
7. A. H. Gandjbakhche, R. F. Bonner, R. Nossal, and G. H. Weiss, "Absorptivity contrast in transillumination imaging of tissue abnormalities," *Appl. Opt.* **35**, 1767 (1996).
8. V. Chernomordik, D. Hattery, A. H. Gandjbakhche, A. Pifferi, P. Taroni, A. Torricelli, G. Valentini, and R. Cubeddu, "Quantification by random walk of the optical parameters of nonlocalized abnormalities embedded within tissuelike phantoms," *Opt. Lett.* **25**, 951 (2000).
9. Y. Painchaud, A. Mailloux, M. Morin, S. Verreault, and P. Beaudry, "Time-domain optical imaging: discrimination between scattering and absorption," *Appl. Opt.* **38**, 3686 (1999).
10. A. Sassaroli, C. Blumetti, F. Martelli, L. Alianelli, D. Contini, A. Ismaelli, and G. Zaccanti, "Monte Carlo procedure for investigating light propagation and imaging of highly scattering media," *Appl. Opt.* **37**, 7392 (1998).
11. M. Morin, S. Verreault, A. Mailloux, J. Frechette, S. Chatigny, Y. Painchaud, and P. Beaudry, "Inclusion characterization in a scattering slab with time-resolved transmittance measurements: perturbation analysis," *Appl. Opt.* **39**, 2840 (2000).
12. J. C. Hebden and S. R. Arridge, "Imaging through scattering media by the use of an analytical model of perturbation amplitudes in the time domain," *Appl. Opt.* **35**, 6788 (1996).
13. V. Chernomordik, R. Nossal, and A. H. Gandjbakhche, "Point spread functions of photons in time-resolved transillumination experiments using simple scaling arguments," *Med. Phys.* **23**, 1857 (1996).
14. V. Chernomordik, D. W. Hattery, D. Grosenick, H. Wabnitz, H. Rinneberg, K. T. Moesta, P. M. Schlag, and A. Gandjbakhche, "Quantification of optical properties of a breast tumor using random walk theory," *J. Biomed. Opt.* **7**(1), 80 (2002).